Available online at www.sciencedirect.com
SCIENCE DIRECT®
Bioorganic & Medicinal Chemistry 13 (2005) 6856–6863
Bioorganic & Medicinal Chemistry

Functional studies on a ketoreductase gene from *Streptomyces* sp. AM-7161 to control the stereochemistry in medermycin biosynthesis

Aiying Li,[a] Takayuki Itoh,[a] Takaaki Taguchi,[b] Ting Xiang,[a] Yutaka Ebizuka[a] and Koji Ichinose[b,*]

[a]*Graduate School of Pharmaceutical Sciences, The University of Tokyo, Hongo, Bunkyo-ku, Tokyo 113-0033, Japan*
[b]*Research Institute of Pharmaceutical Sciences, Musashino University, Shinmachi, Nishitokyo-shi, Tokyo 202-8585, Japan*

Received 16 June 2005; revised 25 July 2005; accepted 26 July 2005
Available online 19 September 2005

Abstract—Medermycin shows the same *trans* (3*S*,15*R*) configuration as actinorhodin in the pyran ring crucial for its bioactivity. One medermycin biosynthetic gene, *med*-ORF12, is assumed to be involved in the stereochemical control at C-3. Functional complementation suggested that it plays a similar role as *act*VI-ORF1 previously proved to determine the stereospecificity at C-3 in actinorhodin biosynthesis. Co-expression of *med*-ORF12 with actinorhodin early biosynthetic genes further demonstrated that *med*-ORF12 encodes a ketoreductase responsible for the enantioselective reduction at C-3 in the formation of the pyran ring.

1. Introduction

The aromatic polyketide medermycin (MED, Fig. 1, **1**), originally isolated from *Streptomyces* sp. K73,[1] is a *C*-glycoside antibiotic with potential therapeutic utility as an anticancer and antibacterial agent.[2–4] MED was highlighted in the first production of 'hybrid' antibiotics by genetic engineering reported by Hopwood et al. in 1985[5] and Ōmura et al. in 1986.[6] MED also includes a number of structural elements to allow studies on interesting biosynthetic problems concerning the polyketide synthases (PKSs),[7] post-PKS ('tailoring') modification,[8] and deoxysugar biosynthesis.[9] In particular, among tailoring steps determining structural diversity in antibiotic biosynthetic pathways, the stereochemical control of a functional group becomes one of the most important medicinal issues related to critical influence on their biological activity. The formation of the two chiral centers at C-3 and C-15 in the pyran ring in MED biosynthesis still has not been studied to date. Thus, it is of high chemical, biological, and pharmacological importance to understand how the stereochemistry is determined in MED biosynthesis, especially, as a step toward metabolic engineering to generate 'unnatural' or 'hybrid' natural products with improved or novel pharmacological profiles in a combinatorial fashion.[7]

MED and actinorhodin (ACT, Fig. 1, **2**), produced by the most genetically characterized polyketide producer, *Streptomyces coelicolor* A3(2),[10] are members of a class of *Streptomyces* aromatic antibiotics known as benzoisochromanequinone (BIQ[11]) antibiotics. All members of BIQs show a *trans* configuration in respect of two chiral centers at C-3 and C-15, which are either (3*S*,15*R*) or (3*R*,15*S*). MED and ACT represent the former type and the opposite stereochemistry is exemplified by dihydrogranaticin (DHGRA, Fig. 1, **3**) produced by *Streptomyces violaceoruber* Tü22.[11–13]

MED, ACT, and DHGRA are proposed to share a common early biosynthetic stage for the generation of the aromatic core structure, followed by different post-PKS modifications (Fig. 1).[7,10–14] The minimal PKS, consisting of the three proteins, ketosynthase (KS), chain length factor (CLF), and acyl carrier protein (ACP), determines a fundamental polyketide chromophore skeleton. The resulting linear polyketide precursor undergoes a C-9 ketoreduction by ketoreductase (KR, defined hereafter as functioning at C-9) followed by cyclization with aromatase (ARO) and cyclase

Keywords: Benzoisochromanequinone antibiotics; Stereospecific ketoreductase; Functional complementation; Heterologous co-expression.
* Corresponding author. Tel./fax: +81 424 68 9184; e-mail: ichinose@musashino-u.ac.jp

0968-0896/$ - see front matter © 2005 Elsevier Ltd. All rights reserved.
doi:10.1016/j.bmc.2005.07.060

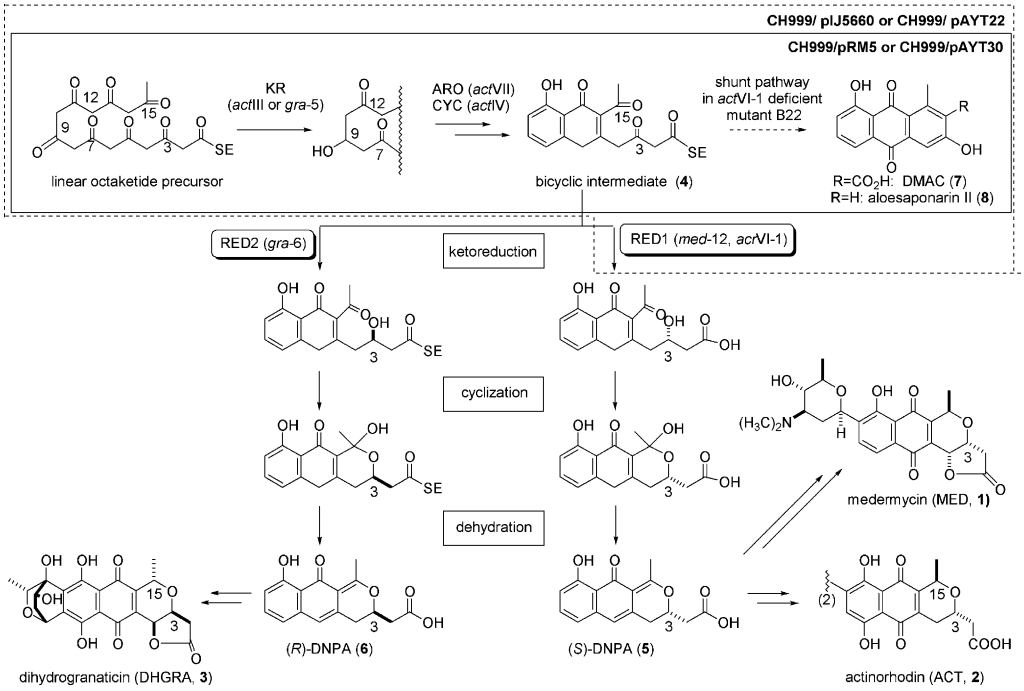

Figure 1. Proposed stereochemical control and a shunt pathway in the biosynthesis of medermycin, actinorhodin, and dihydrogranaticin. Presumed enzyme-bound intermediates are indicated as RCO-SE and shunt products are shown as free acids. Enzymes or putative complexes are shown as capital letters and their encoding genes in parentheses. The bicyclic intermediate is produced by the early biosynthetic enzymes including Min PKS (minimal PKS), KR (ketoreductase for reduction at C-9), ARO (aromatase), and CYC (cyclase), and then is proposed to be stereospecifically reduced by RED1 and 2, defined as stereospecifc ketoreductases for reduction at C-3). Numbering of carbon atoms is based on the biosynthetic origin. pAYT22 and pIJ5660[17] derived from pRM5 are used for co-expression of *act*VI-ORF1 and *med*-ORF12, respectively, together with the *act* early PKS genes. pAYT30 acts as a negative control.

(CYC) to yield a common bicyclic intermediate (Fig. 1, **4**). The subsequent pyran ring formation under the stereochemical control occurs in the tailoring biosynthetic stages, in which the bicyclic intermediate is assumed to be a direct substrate for post modifications at C-3 and C-15.

In the tailoring stage of ACT biosynthesis,[7,10,15] *act*-VI-ORF1 was previously proved to encode a dedicated stereospecific ketoreductase (RED1 type), to establish the (*S*)-configuration at C-3 in the formation of a further advanced chiral intermediate, 4,10-dihydro-9-hydroxy-1-methyl-10-oxo-3-*H*-naphtho-[2,3-*c*]-pyran-3(*S*)-acetic acid, (*S*)-DNPA (Fig. 1, **5**).[16–18] Interestingly, the (*R*)-configuration at C-3 of DNPA (Fig. 1, **6**) in DHGRA biosynthesis was demonstrated to be determined by a *gra*-ORF6 product (RED2 type) which shows no significant similarity to RED1 at the amino acid level.[19,20] Our recent studies showed the remarkable difference between RED1 and RED2 in their substrate specificities as well as in the three-dimensional structures and catalytic mechanisms, though both recognize the same substrate motif of the bicyclic intermediate.[21] Further examples of the related reductases would allow us to understand the unusual mode of stereochemical controls involved in the BIQ antibiotics.

The full sequence of the MED biosynthetic gene cluster cloned from *Streptomyces* sp. AM-7161 reported recently[14] was the third example of the cloning of an entire cluster for BIQ biosynthesis, apart from *act*[16,22,23] and *gra* clusters[12,13] for the biosynthesis of ACT and DHGRA, respectively (Fig. 2), making it available to understand the MED biosynthesis and the mechanism of controlling the stereochemistry by comparative analysis of these gene clusters. We assumed the presence of a RED1 family gene (Fig. 1) in MED biosynthesis to produce (*S*)-DNPA. Similarity searches revealed that *med*-ORF12 shares a high similarity (65%) at the amino acid level with *act*VI-ORF1,[14] making this gene one candidate for study on stereochemical control in MED biosynthetic pathway.

To clarify the stereochemical control during MED biosynthesis, we have investigated here the function of *med*-ORF12 with complementation and co-expression approaches and elucidated its involvement in the formation of the chiral center at C-3 in the pyran ring.

2. Results

2.1. Comparative analysis of proposed ketoreductase genes in *act*, *gra*, and *med* clusters

The crucial role of multiple ketoreductase activities in establishing the diversity of chemistry and stereochemistry of the PKS products allowed our present study to focus initially on the analysis of genes potentially responsible for the reduction either at C-3 or C-9 in MED biosynthesis. KRs functioning at C-9 of aromatic

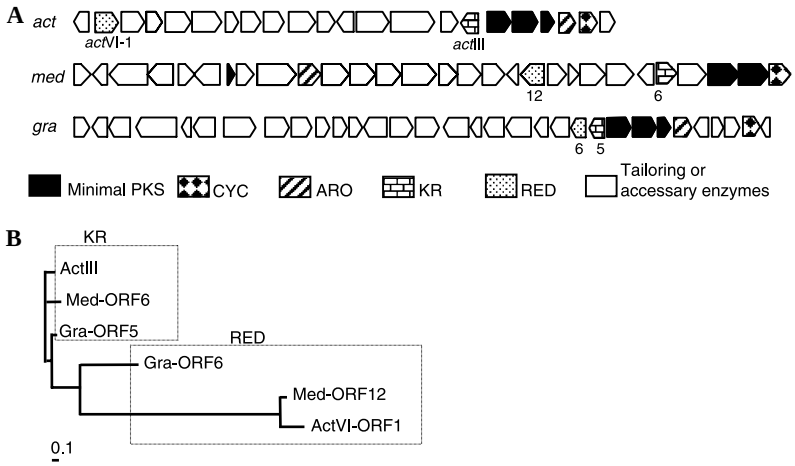

Figure 2. (A) Genetic organization of *act*, *med*, and *gra* gene clusters. The numbering in bold indicates the proposed ketoreductase genes; (B) phylogenetic tree of six proposed ketoreductases in three BIQ biosynthetic pathways. The indicated scale represents 0.1 amino acid substitution per site. Six ketoreductases are grouped into KR and RED families (see Fig. 1), respectively. The entries of the sequences (protein Accession No.): ActIII (AAA26688), ActVI-ORF1 (CAA44233), Gra-ORF5 (CAA09652), Gra-ORF6 (CAA09651), Med-ORF6 (BAC79042), and Med-ORF12 (BAC79036).

polyketide intermediates are highly homologous (>70%) in numerous type II PKS systems. All of them belong to typical short-chain alcohol dehydrogenases/reductases (SDRs)[7,24] and are exemplified in the BIQ systems by products of *act*III[22] for ACT and *gra*-ORF5[12,13,19,20] for DHGRA. The two putative ketoreductase genes (*med*-ORF6 and *med*-ORF12) were also found in the *med* cluster.[14] The *med*-ORF12 product sharing a rather high homology with ActVI-ORF1 (65/57%)[14] was further classified into a dehydrogenase with a specific function as a 3-hydroxyacyl CoA dehydrogenase (3HAD) essential for β-oxidation of fatty acids. No significant similarity was found between Med-ORF12 and Gra-ORF6 (as defined by the BLAST2 Sequences program), though both are proposed to recognize the same substrate (Fig. 1). Phylogenetic analysis in Figure 2 shows that the RED members, Med-ORF12, ActVI-ORF1, and Gra-ORF6, occupy a distinguished position from the KRs including Med-ORF6, ActIII, and Gra-ORF5, convincingly supporting our putative functional assignments of the reductase genes.

2.2. Complementary analysis of *med*-ORF12 in *act*VI-ORF1-deficient strain

The initial trial to confirm the involvement of *med*-ORF12 in the formation of a chiral center at C-3 in MED biosynthesis was its expression in the *act*VI-ORF1-deficient mutant, *S. coelicolor* B22,[25] to investigate whether it could complement the functional mutation of *act*VI-ORF1. Plasmid pAYT19 was designed for expression of *med*-ORF12 under the control of a thiostrepton-inducible promoter, *tip*Ap, carried by pIJ8600.[26] PEG-assisted delivery into B22, as described previously,[26] was followed by the treatment with apramycin and thiostrepton to select transformants. Plasmid integration into the chromosome of B22 was confirmed by PCR amplification with genomic DNA of transformants as templates (data not shown). The inducibility of *med*-ORF12 expression in the recombinant B22/pAYT19 was tested in the liquid culture with or without addition of thiostrepton (12.5 μg/mL). The typical pH indicator properties of ACT (red under acidic conditions and blue under basic ones) allow carrying out a simple complementation test using pigmentation to reveal ACT production.

Successful complementation of *act*VI-ORF1 mutation was observed with pAYT19: the broth of recombinant strain B22/pAYT19 under the thiostrepton induction gave a blue pigmentation, which turned into red after acid treatment, as well as wild type strain, M145, implying the accumulation of ACT as a result of the expression of *med*-ORF12, whereas B22/pAYT19 without addition of thiostrepton failed to produce a blue pigment, showing the same phenotype with mutant B22 (Fig. 3A). The culture of B22/pAYT19 was also analyzed by LC/ESI/MS measurement under previous conditions.[18] The quite efficient accumulation of ACT in the mycelium could be detected (Figs. 3B and C) under the induced conditions and two shunt products, DMAC (Fig. 1, **7**) and aloesaponarin II (Fig. 1, **8**),[27,28] disappeared (data not shown), indicating that the common bicyclic intermediate in B22/pAYT19 was further metabolized into ACT, likely, with the assistance of *med*-ORF12 expressed under the induced conditions.

2.3. Co-expression of *med*-ORF12 with *act* early PKS genes

To further characterize the function of *med*-ORF12 relevant to the configuration at C-3 in MED biosynthesis, co-expression in vivo of *med*-ORF12 with an early-*act*-PKS-gene cassette consisting of *act* minimal PKS (KS, CLF, and ACP), KR, ARO, and CYC genes was explored to clarify whether the common bicyclic intermediate was converted into (*S*)-DNPA by a stereospecific reduction of the carbonyl group at C-3 in the presence of *med*-ORF12.

One expression plasmid based on this gene cassette provided by pRM5,[28] was designed to be added by

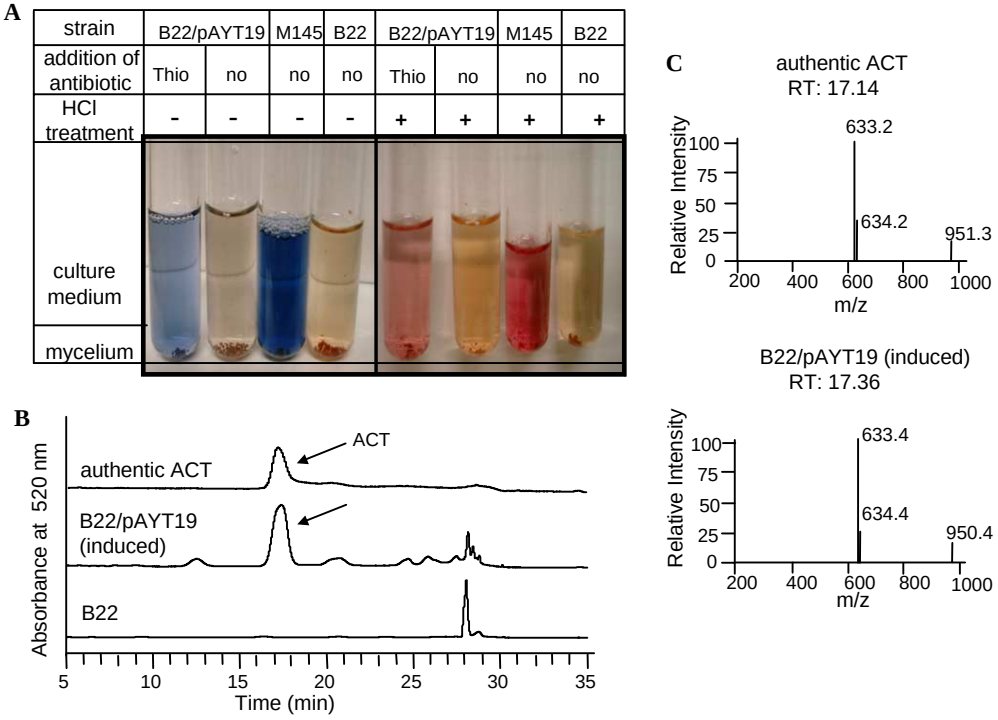

Figure 3. (A) Phenotypic characterization of *S. coelicolor* M145 and B22, and its transformants. Thio/no: with or without addition of thiostrepton (12.5 μg/mL) into R4 culture for induction. Two milliliters aliquot was sampled out from *Streptomyces* cultures into a test tube and subjected to acid treatment: +, addition of 200 μL of 1 N HCl; −, addition of 200 μL of deionized water; (B) HPLC profiles (absorbance at 520 nm) of metabolites of *S. coelicolor* B22 and its recombinants; (C) MS spectra of the peaks corresponding to the authentic ACT and B22/pAYT19 product indicated by arrows.

med-ORF12 and expressed in *S. coelicolor* CH999, an *act*-deficient mutant.[28] The *act* early PKS genes on pRM5 are required to produce the bicyclic intermediate, that undergoes further spontaneous cyclization to produce shunt products, DMAC and aloesaponarin II (Fig. 1). The initial trial by adding of *med*-ORF12 into pRM5 system to generate pAYT3 and delivering it into CH999 failed due to the gene rearrangement occurring in CH999 (data not shown). Therefore, a new expression plasmid, designated as pAYT22 (Fig. 1), was constructed by delivering the same gene cassette released from pAYT3 consisting of *act* early PKS genes together with an additional *med*-ORF12 into an integrative vector, pSET152.[26]

LC/APCI/MS measurement (Figs. 4A and B) demonstrated that the new *S. coelicolor* recombinant strain, CH999/pAYT22, produced a high amount of DNPA with the same retention time, characteristic absorbance pattern (data not shown), and molecular weight with authentic (*S*)-DNPA produced by CH999/pIJ5660 consisting of *act*VI-ORF1 and same *act* early PKS genes (Fig. 1).[17] It was also observed that the amount of two shunt products, DMAC and aloesaponarin II, was markedly decreased in CH999/pAYT22, as well as in CH999/pIJ5660, whereas the negative control, CH999/pAYT30, failed to produce (*S*)-DNPA due to the absence of *med*-ORF12, indicating that DNPA in CH999/pAYT22 is derived from the common bicyclic intermediate that undergoes specific reduction at the C-3 keto-group in the expression of *med*-ORF12.

2.4. Stereochemistry at C-3 of DNPA produced by *med*-ORF12

The configuration at C-3 of DNPA produced by CH999/pAYT22 was proved by the chiral HPLC analysis. The large-scaled culture of CH999/pAYT22 extracted with chloroform was subjected to silica-gel column chromatography and further preparative HPLC for purification of DNPA, which was used for chiral HPLC analysis on the configuration at C-3.[20] Figure 4C shows the clear difference (>1 min) in retention time between authentic (*S*)-DNPA and (*R*)-DNPA.[20] Under the same conditions, DNPA produced by CH999/pAYT22 gave a single peak with a similar retention time with authentic (*S*)-DNPA, suggesting that the product of CH999/pAYT22 is DNPA with a specific (*S*)-configuration at C-3 without any trace of (*R*)-DNPA. This result further confirmed that *med*-ORF12 protein in the co-expression system of pAYT22 reduces stereospecifically the common bicyclic intermediate to establish the (*S*)-configuration at C-3 of the pyran ring and lead to an accumulation of (*S*)-DNPA (Fig. 1).

3. Discussion

3.1. Role of Med-ORF12

Mechanistically, most of the post-PKS tailoring steps for the aglycone formation in MED biosynthesis were expected to follow the ACT pathway.[14] Observation

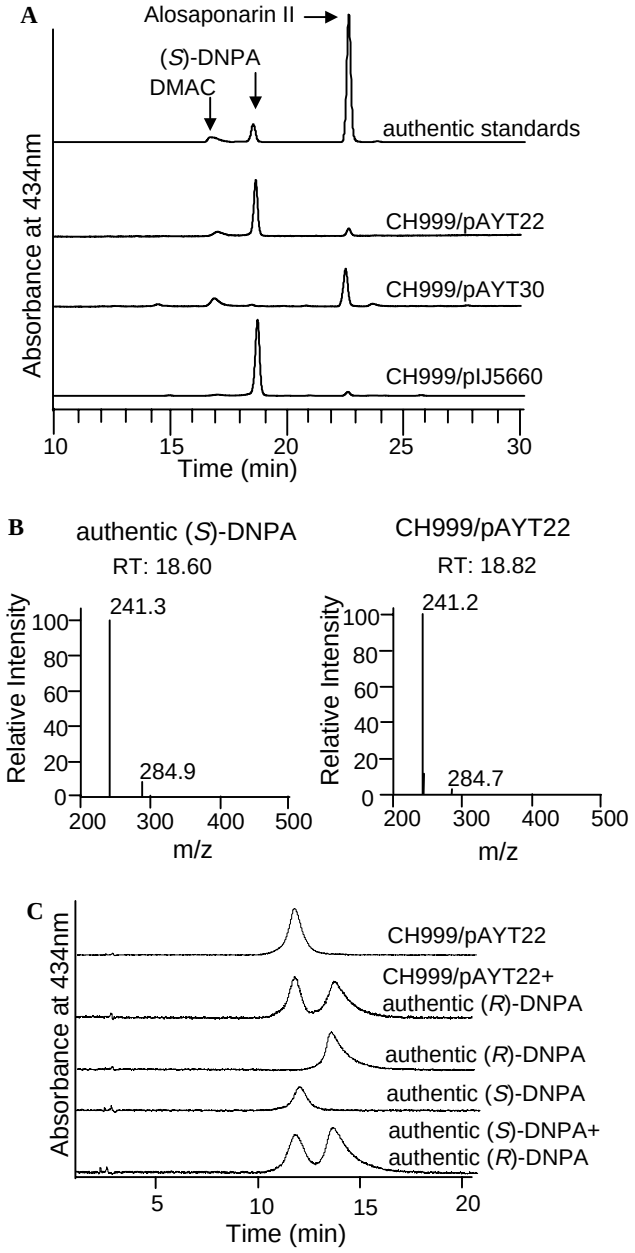

Figure 4. (A) HPLC profiles (absorbance at 434 nm) of metabolites of *S. coelicolor* CH999 recombinants; (B) MS spectra of the peaks corresponding to the authentic (*S*)-DNPA and the main product of CH999/pAYT22; (C) chiral HPLC profiles of DNPAs including authentic (*R*)- and (*S*)-samples (see text for the details of each chromatogram).

of *med*-ORF12 sharing a high similarity with *act*VI-ORF1 critical in the ACT biosynthetic pathway provided a clue to study the stereochemical control in MED biosynthesis. Based on the fact that the common bicyclic intermediate was reduced into DNPA with the definite (3*S*) configuration, assisted by *med*-ORF12, *med*-ORF12 was suggested to encode a stereospecific ketoreductase the same as the *act*VI-ORF1 product to recognize the common bicyclic intermediate as its substrate. The present results clearly demonstrated a MED biosynthetic gene, *med*-ORF12, is involved in the stereochemical control in the formation of the pyran ring in the MED biosynthetic pathway. This study provides the second example of functionally proved RED1 family reductases in the BIQ biosynthesis, allowing further mechanistic study on an interesting biosynthetic problem of the opposite stereochemical controls by ketoreductases with virtually no similarity to either sequences[20] or gross three-dimensional structures.[21]

Co-expression of genes of interest with the *act* early PKS gene cassette carried by pRM5 in CH999 is one commonly used strategy to perform functional analysis, especially on tailoring PKS genes. However, in our initial trial using a direct derivative from pRM5 and expressing it in CH999, plasmid DNA was not able to maintain stably in CH999 due to the gene rearrangement. Co-expression system in CH999 finally was accomplished functionally using the integrative vector, pSET152, and yielded a comparable amount of (*S*)-DNPA in CH999/pAYT22, together with a still detectable production of the shunt products, DMAC and aloesaponarin II, as well as in CH999/pIJ5660. Generally, the amount of (*S*)-DNPA in CH999/pAYT22 is still slightly lower than that in CH999/pIJ5660 probably due to the possible presence of an 'unnatural' combination of enzymes between heterologous Med-ORF12 and *act* early PKSs to lead to less efficient enzymatic reaction than that between native RED1 (ActVI-ORF1) and *act* early PKSs. Another possibility for lower but efficient production of (*S*)-DNPA in CH999/pAYT22 is the lower copy number of pAYT22 integrated into the host genome than autonomously replicative pRM5 derivatives.

3.2. Comparison between Med-ORF12, ActVI-ORF1, and Gra-ORF6

Based on sequence comparison and phylogenetic analysis, three REDs in BIQ biosynthesis were proposed to be classified into two types (RED1 and RED2) without any mutual homology, although all of them recognize the same substrate motif. This is different from the case for tropinone reductases I and II (TR-I and TR-II) sharing 64% identity at the amino acid level and well-conserved overall structures and recognizing a common alkaloid intermediate, tropinone, as their substrate to yield 3α- or 3β-hydroxytropane, respectively. The presence of different charged residues in TR-1 and TR-II was proposed to contribute controlling the binding orientation of tropinone to determine the stereospecificity of the reaction product.[29]

PSI-BLAST analysis categorized more specifically RED1 into 3HAD which reversibly catalyzes the β-oxidation of the hydroxyl group of L-3-hydroxyacyl-CoA with a partially similar structure to the reactive portion of the bicyclic intermediate,[30] whereas RED2 comes under the category of SDR with expected characteristic sequence patterns.[20,21]

Recent investigations revealed the obvious difference of proposed catalytic mechanisms of these two types of REDs, based on homodimer models: in the case of

```
3HAD     151 QDRFAGLHFF NPVPVMKLVE VIKTPMT 177

ActVI-1  122 PGRLVVAHPF NPPHIVPLVE VVRGERT 148

Med-12   134 SGRLVVGHPF NSPHIVPLVE VVGGERT 160
```

Figure 5. Sequence alignment of the conserved regions between 3HAD, ActVI-ORF1 (ActVI-1), and Med-ORF12 (Med-12). Conserved residues are in bold and the key catalytic residues are marked with bold underline. The numbers indicate amino acid positions of each entry.

RED1, the appropriate interaction between His^{129} and Glu^{141} is essential for the reduction of the C-3 keto group by the proton of His^{129} and for transferring *pro-S* proton of nicotinamide of cofactor NAD(P)H to C-3 of the bicyclic intermediate, whereas, in the case of RED2, the Ser^{144}-Tyr^{157}-Lys^{161} triad performs an essential role for its acid–base catalysis, in which Lys^{161} and Tyr^{157} are hydrogen bonded to both 2′- and 3′-hydroxy groups of nicotinamide of NAD(P)H to allow transferring *pro-S* proton of nicotinamide of NAD(P)H to the substrate.[21]

Further alignment of the amino acid sequences of the RED1-type proteins with 3HAD indicated that highly conserved residues, including the proposed His-Glu catalytic dyad,[30–32] are present in Med-ORF12 (Fig. 5), implying that Med-ORF12 might perform its reducing activity to give the (*S*)-configuration at C-3 of DNPA in a similar catalytic mechanism to ActVI-ORF1.

3.3. Proposed evolution of Med-ORF12

The present functional analysis convincingly proved the similar role between ActVI-ORF1 and Med-ORF12. The same stereospecific reducing activity, high resemblance at the amino acid level, and well-conserved catalytic residues imply that they might share a common evolutional origin, although they are present in different bacterial strains.

3HADs are critical for the β-oxidation of short chain fatty acids in primary metabolisms, and are widely distributed in nature. Particularly, nine homologues of 3HAD were found on the genome of ACT-producing *S. coelicolor*.[33] The origin of ActVI-ORF1 was proposed to be deduced from one copy of 3HAD somewhere else on the genome of *S. coelicolor*, which was inserted into the *act* gene cluster with mutation and acquired the reduction activity of the bicyclic intermediate.[21] Therefore, it could be hypothetical that Med-ORF12 might undergo a similar evolutionary route, probably also deduced from 3HAD. Furthermore, the sequence identity (18%) between Med-ORF12 and 3HAD is lower than that (24%) between ActVI-ORF1 and 3HAD, implying that Med-ORF12 was evolved farther than ActVI-ORF1 if they had originated from a common ancestor.

4. Conclusion

Toward metabolic engineering of an increasing number of polyketide antibiotic biosynthetic gene clusters to generate 'unnatural' natural compounds for effective therapeutics, a better functional understanding of each tailoring enzyme is critically important. The stereochemical control in BIQ biosynthetic pathways is one of the most important tailoring modifications to determine their bioactivity. We clarified here one key stereospecific ketoreductase encoded by *med*-ORF12 in the medermycin biosynthetic gene cluster, which catalyzes the enantioselective ketoreduction at C-3 of the bicyclic intermediate to control the (3*S*) configuration in the pyran ring, based on the facts of functional complementation of *act*VI-ORF1 mutation with *med*-ORF12 and (*S*)-DNPA accumulation by co-expression of *med*-ORF12 together with *act* early PKS genes. Furthermore, the present result is one of the key frameworks to understand a new example of opposite stereochemical controls in antibiotic biosynthesis to provide diverse chiral metabolites.

5. Experimental procedures

5.1. Bacterial strains, plasmids, and culture conditions

Streptomyces strains in this study are ACT-producing *S. coelicolor* M145 as a wild type control[26] and an *act*VI-ORF1-deficient strain, *S. coelicolor* B22,[25] and an *act*-cluster-deficient mutant, *S. coelicolor* CH999,[28] used for recombinant expression. pT7Blue T-vector was obtained from Novagen for PCR cloning. pIJ226, as a template for amplification of *med*-ORF12 by PCR, is a subclone carrying a 2.3 kb *Bam*HI genetic fragment from pIK340 used for sequencing of the *med* gene cluster.[14] pIJ8600[26] contains the *tip*A promoter used for induced expression of *med*-ORF12 in *S. coelicolor* B22. pRM5[28] provides an expression cassette consisting of *act* early PKS genes for the production of a common bicyclic intermediate in the early stage of ACT biosynthetic pathway (Fig. 1). pSET152[26] acts as an integrative vector for the construction of expression plasmids. *Streptomyces* strains were maintained on R4,[21] SFM, or GYM agar medium and grown in YEME or TSB liquid medium.[26] The production cultures of *Streptomyces* recombinant strains were liquid-inoculated in R4 liquid medium, according to previous procedures.[21,34]

5.2. Computer analysis of DNA and protein sequences

Sequence comparison was performed with updated BLAST programs online (PSI-BLAST, BLAST2 Sequences, and rpsBLAST). Phylogenetic analysis of protein sequences was conducted with the clustalw program provided by DDBJ (http://www.ddbj.nig.ac.jp/search/clustalw), based on a neighbor-joining method and a phylogenetic tree was created with the TreeView program (version 1.6.2, freely available from the Taxonomy and Systematics server at the University of Glasgow, UK).

5.3. General genetic manipulations

PEG-assisted transformation with *Streptomyces* protoplast and genomic DNA isolation from *Streptomyces* strains were described previously.[26] General molecular biology manipulations were performed as described by Sambrook et al.[35] DNA amplification by PCR with Ex Taq (TaKaRa) kit was conducted in the RoboCycler® Gradient 40 (Stratagene®) using a step program (0.5 min at 94 °C, 0.5 min at 68 °C and 1 min at 72 °C), according to the manufacturer's protocol, except for the addition of 5% of DMSO. Three primers used in PCRs were designed using the GenBank data (accession number is AB103463) and obtained from Nihon Bioservice (Saitama, Japan): (1) Med12S-NdeI (5′-C**CATATG** AGCGGAACCGGCCGGC; underline, *Nde*I site; bold, start codon); (2) Med12S-Sp (5′-ACATGCATGCAT *GGGAG*AACGAAAACG**ATG**AGCGG AAC; underline, *Sph*I; bold, start codon; italic, ribosome-binding site, RBS); 3. Med12A-Bam-EI (5′-CG GGATCCCG GAATTCCGGCGCCC**TCA**CGA CGC GCTCC; first underline, *Bam*HI site; second underline, *Eco*RI site; bold, stop codon).

5.4. Construction of expression plasmids

A 980 bp-encoding region of *med*-ORF12 amplified by PCR with Med12S-NdeI and Med12A-Bam-EI primers was inserted into the *Nde*I-*Bam*HI sites downstream of *tip*A promoter on pIJ8600 to generate the recombinant plasmid, pAYT19, which was subsequently introduced into *S. coelicolor* B22 for complementation experiment. Additionally, the same encoding region of *med*-ORF12 amplified by PCR with Med12S-Sp and Med12A-Bam-EI primers was used to replace *act*VI-ORF1 on pIJ5660[17] derived from pRM5 to yield pAYT3. The entire *Hind*III-*Eco*RI fragment containing *act* early PKS genes and *med*-ORF12 released from pAYT3 was blunted with Klenow digestion and inserted into the *Eco*RV site of pSET152. The expression plasmid thus obtained was designated as pAYT22. As a negative control, pAYT30 was constructed by ligating *Hind*III-*Eco*RI fragment released from pRM5 with pSET152. pAYT22 and pAYT30 were then used to transform *S. coelicolor* CH999.

5.5. LC/MS analysis for ACT and DNPA

The mycelia of *S. coelicolor* strains were extracted with 1,4-dioxane, as described by Taguchi et al.[18] Crude extracts were subjected to LC/ESI/MS analysis on HP1100 series/LCQ system by monitoring the absorbance of ACT at 520 nm using a reversed-phase column, Luna C18 (4.6 mm i.d. × 150 mm, Phenomenex), maintained at 40 °C, and eluted with aq CH_3CN containing 0.5% AcOH as the following gradient profile: 0–25 min, 44%; 25–28 min, 44–60%; 28–30 min, 60–95%; 30–32 min, 95%; and 32–35 min, 95–44%. Samples for DNPA measurements were prepared from R4 liquid cultures of *S. coelicolor* strains, the supernatants of which were extracted with EtOAc and then subjected to the LC/APCI/MS analysis on HP1100 series/LCQ system under the conditions previously described.[18,20]

5.6. Isolation, purification, and chiral HPLC analysis of DNPA

The supernatants were harvested from 2 L-scaled R4 liquid cultures of *Streptomyces* strains and extracted twice with chloroform. DNPAs were purified from the crude extracts by silica gel column chromatography and then preparative HPLC according to previous descriptions.[20]

Chiral HPLC analysis of DNPAs purified from the *Streptomyces* strains was performed on a TOSOH 8020 system with a chiral column, TSK gel Enantio-OVM (4.6 mm i.d. × 150 mm, TOSOH), under the established conditions.[20]

Acknowledgments

A.L. was a recipient of Japan Society for the Promotion of Science (JSPS) Postdoctoral Fellowship For Foreign Researcher (P03308). Part of this work was supported by MEXT. HAITEKU (2004). We are grateful to Prof. Dr. Jörn Piel for helpful discussion.

References and notes

1. Takano, S.; Hasuda, K.; Ito, A.; Koide, Y.; Ishii, F.; Haneda, I.; Chihara, S.; Koyama, Y. *J. Antibiot.* **1976**, *29*, 765.
2. Tanaka, N.; Okabe, T.; Isono, F.; Kashiwagi, M.; Nomoto, K.; Takahashi, M.; Shimazu, A.; Nishimura, T. *J. Antibiot.* **1985**, *38*, 1327.
3. Tatsuta, K.; Ozeki, H.; Yamaguchi, M.; Tanaka, M.; Okui, T. *Tetrahedron Lett.* **1990**, *31*, 5495.
4. Okabe, T.; Nomoto, K.; Funabashi, H.; Okuda, S.; Suzuki, H.; Tanaka, N. *J. Antibiot.* **1985**, *38*, 1333.
5. Hopwood, D. A.; Malpartida, F.; Kieser, H. M.; Ikeda, H.; Duncan, J.; Fujii, I.; Rudd, B. A. M.; Floss, H. G.; Ōmura, S. *Nature* **1985**, *314*, 642.
6. Ōmura, S.; Ikeda, H.; Malpartida, F.; Kieser, H. M.; Hopwood, D. A. *Antimicrob. Agents Chemother.* **1986**, *29*, 13.
7. Hopwood, D. A. *Chem. Rev.* **1997**, *97*, 2465.
8. Rix, U.; Fischer, C.; Remsing, L. L.; Rohr, J. *Nat. Prod. Rep.* **2002**, *19*, 542.
9. Trefzer, A.; Salas, J. A.; Bechthold, A. *Nat. Prod. Rep.* **1999**, *16*, 283.
10. Hopwood, D. A. *Microbiology* **1999**, *145*, 2183.
11. Ichinose, K.; Taguchi, T.; Ebizuka, Y.; Hopwood, D. A. *Actinomycetologica* **1998**, *12*, 99.
12. Sherman, D. H.; Malpartida, F.; Bibb, M. J.; Kieser, H. M.; Bibb, M. J.; Hopwood, D. A. *EMBO. J.* **1989**, *8*, 2717.
13. Ichinose, K.; Bedford, D. J.; Tornus, D.; Bechthold, A.; Bibb, M. J.; Revill, W. P.; Floss, H. G.; Hopwood, D. A. *Chem. Biol.* **1998**, *5*, 647.
14. Ichinose, K.; Ozawa, M.; Itou, K.; Kunieda, K.; Ebizuka, Y. *Microbiology* **2003**, *149*, 1633.
15. Cole, S. P.; Rudd, B. A. M.; Hopwood, D. A.; Chang, C. J.; Floss, H. G. *J. Antibiot.* **1987**, *40*, 340.
16. Fernández-Moreno, M. A.; Martinez, E.; Caballero, J. L.; Ichinose, K.; Hopwood, D. A.; Malpartida, F. *J. Biol. Chem.* **1994**, *269*, 24854.
17. Ichinose, K.; Surti, C.; Taguchi, T.; Malpartida, F.; Booker-Milburn, K. I.; Stephenson, G. R.; Ebizuka, Y.; Hopwood, D. A. *Bioorg. Med. Chem. Lett.* **1999**, *9*, 395.

18. Taguchi, T.; Itou, K.; Ebizuka, Y.; Malpartida, F.; Hopwood, D. A.; Surti, C. M.; Booker-Milburn, K. I.; Stephenson, G. R.; Ichinose, K.. *J. Antibiot.* **2000**, *53*, 144.
19. Ichinose, K.; Taguchi, T.; Bedford, D. J.; Ebizuka, Y.; Hopwood, D. A. *J. Bacteriol.* **2001**, *183*, 3247.
20. Taguchi, T.; Ebizuka, Y.; Hopwood, D. A.; Ichinose, K. *J. Am. Chem. Soc.* **2001**, *123*, 11376.
21. Taguchi, T.; Kunieda, K.; Takeda-Shitaka, M.; Takaya, D.; Kawano, N.; Kimberley, M. R.; Booker-Milburn, K. I.; Stephenson, G. R.; Umeyama, H.; Ebizuka, Y.; Ichinose, K. *Bioorg. Med. Chem.* **2004**, *12*, 5917.
22. Hallam, S. E.; Malpartida, F.; Hopwood, D. A. *Gene* **1988**, *74*, 305.
23. Fernández-Moreno, M. A.; Martinez, E.; Boto, L.; Hopwood, D. A.; Malpartida, F. *J. Biol. Chem.* **1992**, *267*, 19278.
24. Persson, B.; Krook, M.; Jörnvall, H. *Eur. J. Biochem.* **1991**, *200*, 537.
25. Rudd, B. A. M.; Hopwood, D. A. *J. Gen. Microbiol.* **1979**, *114*, 35.
26. Kieser, T.; Bibb, M. J.; Buttner, M. J.; Chater, K. F.; Hopwood, D. A. *Practical Streptomyces Genetics*; The John Innes Foundation: Norwich, UK, 2000.
27. Bartel, P. L.; Zhu, C. B.; Lampel, J. S.; Dosch, D. C.; Conners, S. P.; Strohl, W. R.; Beale, J. M.; Floss, H. G. *J. Bacteriol.* **1990**, *172*, 4816.
28. McDaniel, R.; Ebert-Khosla, S.; Hopwood, D. A.; Khosla, C. *Science* **1993**, *262*, 1546.
29. Nakajima, K.; Yamashita, A.; Akama, H.; Nakatsu, T.; Kato, H.; Hashimoto, T.; Oda, J.; Yamada, Y. *Proc. Natl. Acad. Sci. U.S.A.* **1998**, *95*, 4876.
30. Barycki, J. J.; O'Brien, L. K.; Bratt, J. M.; Zhang, R.; Sanixhvili, R.; Strauss, A. W.; Banaszak, L. J. *J. Biochemistry* **1999**, *38*, 5786.
31. Barycki, J. J.; O'Brien, L. K.; Strauss, A. W.; Banaszak, L. J. *J. Biol. Chem.* **2000**, *275*, 27186.
32. Barycki, J. J.; O'Brien, L. K.; Strauss, A. W.; Banaszak, L. J. *J. Biol. Chem.* **2001**, *276*, 36718.
33. Bentley, S. D.; Chater, K. F.; Cerdeno-Tarraga, A. M.; Challis, G. L.; Thomsom, N. R.; James, K. D.; Harris, D. E.; Quail, M. A.; Kieser, H.; Harper, D.; Bateman, A.; Brown, S.; Chandra, G.; Chen, C. W.; Collins, M.; Cronin, A.; Fraser, A.; Goble, A.; Hidalgo, J.; Homsby, T.; Howarth, S.; Huang, C. H.; Kieser, T.; Larke, L.; Murphy, L.; Oliver, K.; O'Neil, S.; Rabbinowitsch, E.; Rajandream, M. A.; Rutherford, K.; Rutter, S.; Seeger, K.; Saunders, D.; Sharp, S.; Squares, R.; Squares, S.; Taylor, K.; Warren, T.; Wietzorrek, A.; Woodward, J.; Barell, B. G.; Parkhill, J.; Hopwood, D. A. *Nature* **2002**, *417*, 141.
34. Ozawa, M.; Taguchi, T.; Itoh, T.; Ebizuka, Y.; Booker-Milburn, K. I.; Stephenson, G. R.; Ichinose, K. *Tetrahedron* **2003**, *59*, 8793.
35. Sambrook, J.; Fritsch, E. F.; Maniatis, T. *Molecular Cloning: A Laboratory Manual*, 2nd ed.; Cold Spring Harbor Laboratory: Cold Spring Harbor, NY, 1989.